

Simulation verification of influence of biological tissue structure on shear wave velocity evaluation

Kodai Osato^{1†}, Takuma Oguri², Naohisa Kamiyama², Shinnosuke Hirata³, Kenji Yoshida³ and Tadashi Yamaguchi³ (¹ Grad. School Sci. and Eng. Chiba Univ.; ² Ultrasound General Imaging, GE Healthcare; ³ Center for Frontier Medical Engineering, Chiba Univ.)

1. Introduction

Shear wave elastography (SWE) is a diagnostic method that non-invasively measures the stiffness of living tissues, and is considered to be an index for lesion detection and specific diagnosis. In recent years, it has begun to be applied to muscles, but it has been suggested that the evaluation accuracy of shear wave velocity (SWV) differs depending on the positional relationship between the propagation direction and the running direction of the muscles. In addition, there is a possibility that the acoustic radiation force (ARF) may not be input as expected in a tissue with strong anisotropy¹.

In this study, shear waves propagating in biological tissue were simulated by the elastic finite difference time domain (FDTD) method² under transmission conditions mimicking distribution of acoustic radiation force (ARF) in a clinical diagnostic system. The effect of SWV evaluation when ARF is not applied to the muscle and liver as expected was examined.

2. Method

2.1 Simulation

Figure 1 shows the schematic images of simulation spaces. The ARF and shear wave propagating in the simulation space (50 mm × 60 mm; 1 pixel = 10 μm) were simulated using the elastic FDTD method. The focus depth of the ARF was 30 mm, and the transmission conditions simulated the push pulse of abdominal linear array probe (9L-D, GE Healthcare) of ultrasonic equipment (LOGIQ S8, GE Healthcare). As shown in **Fig. 1(B)**, by placing the fatty layer on the propagation path of the ARF, a case in which the irradiation condition of the ARF was different from those assumed was also reproduced.

The 10 mm × 10 mm area in the simulation space (light blue area in **Fig. 1**) was placed the long and short axis that were reproduced from pathological images of actual muscles. The simulation models of long and short axis are shown in **Fig. 2**. The SWVs were set at 3 m/s for muscle fibers and 1 m/s for membranes.

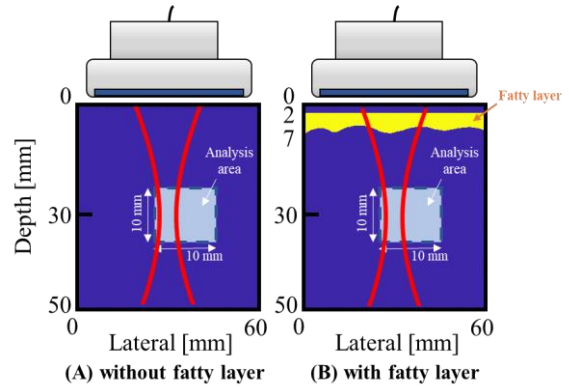


Fig. 1 Schematic images of simulation spaces

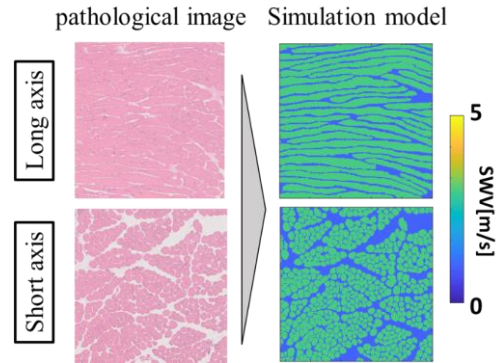


Fig. 1 Muscle mimicked simulation models

2.2 SWV evaluation

The propagation time difference τ of the shear wave was calculated by the cross-correlation method in the time waveform of two points on the spatial grid adjacent to each other in the lateral direction. At the time of calculation, a Tukey window with 1.5 times the wavelength was applied. The cross-correlation function $R(\tau)$ was calculated as

$$R(\tau) = \int v_1(t) \cdot v_2(t + \tau) dt \quad (1)$$

where the v_1 and v_2 are the time waveforms of the particle velocities in the depth direction at two consecutive points in the lateral direction, respectively. The shear wave propagation time difference τ is the time when $R(\tau)$ is maximum.

The SWV was calculated as

$$SWV(x, y) = \frac{\Delta x}{\tau} \quad (2)$$

where the propagation time difference τ and the

[†]osato@chiba-u.jp, *yamaguchi@faculty.chiba-u.jp

distance Δx between the spatial grids between two adjacent points. The SWVMAP in the analysis area was created by calculating in each spatial grid³.

3. Results

Figure 3(a) show the ARF propagations, wavefronts of shear wave propagation, and SWVMAPs in the long axis of muscle. In the ARF without the fatty layer shown in the upper row, the propagation of the shear wave is stable. By contrast, in the ARF with the fatty layer shown in the lower row, the ARF does not focus as expected, and the wavefronts of shear wave propagate disturbed. Because of these wavefront disturbance effects, the SWV values are calculated to be higher in general with the fatty layer than without the fatty layer as shown in **Fig. 3(b)**.

Figure 4(a) shows the results for the short axis of muscles. The wavefronts of the shear wave in the short axis are disturbed significantly with the elapse of time compared with the case of the long axis. This is because there are many boundary surfaces between muscle fibers and membranes with the short axis perpendicular to the direction of shear wave propagation, and they are affected by reflections from these boundary surfaces. In the ARF with a fatty layer, the wavefronts of the shear wave propagation are more disturbed than in the ARF without a fatty layer, as in the long axis. In the short axis, in addition to wavefronts disturbance, refraction caused by the shape of muscle fibers strongly affected the SWV values, resulting in a large variation and a large difference from the theoretical values as shown in **Fig. 4(b)**.

4. Conclusion

Elastic FDTD simulations were used to verify the relationship between ARF conditions and SWV evaluation, as well as the relationship between different muscle tissue structures and SWV evaluation. When the propagation path of longitudinal waves contains layers with significantly different acoustic properties, the irradiation conditions of the ARF can easily deviate from those assumed, suggesting that the accuracy of SWV estimation may be significantly reduced due to the influence of tissue structure.

Currently, detailed verification of the accuracy of SWV evaluation is being promoted for a model in which multiple types of biological tissues form a multi-layered structure between the body surface and the tissue to be evaluated inside the body.

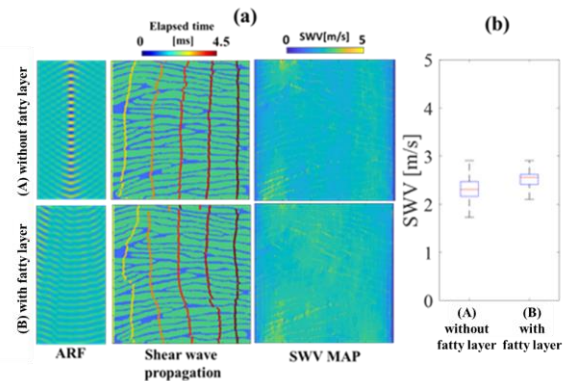


Fig. 3 Simulation results of shear wave propagation in long axis. (a) ARF propagations, wavefronts of shear wave propagation, and SWVMAPs, (b) boxplot of evaluated SWVs.

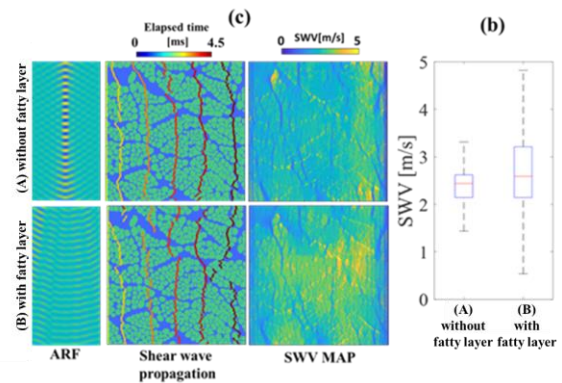


Fig. 4 Simulation results of shear wave propagation in short axis. (a) ARF propagations, wavefronts of shear wave propagation, and SWVMAPs, (b) boxplot of evaluated SWVs.

Acknowledgment

This work was partly supported by JSPS Core-to-Core Program, JPJSCCA2017000, the Institute for Advanced Academic Research at Chiba University.

References

1. Palmeri M.L., et al; *IEEE TUFFC*, **64** (2017)
2. Sato. M, *Introduction to analysis of elastic vibration and wave motion by FDTD method*, Morishita Publishing (2003) [in Japanese]
3. Yamakawa M, *Med. Image. Tech.*, **32** (2014)